

Non-Resonant Kinetic Energy Harvesting using Macro-Fiber Composite Patch

Giulia Bassani, *Student, IEEE* Alessandro Filipeschi, *Member, IEEE* Emanuele Ruffaldi, *Member, IEEE*

Abstract—Over the past decades, thanks to the progresses being made in low power microelectronics, wireless technology, and energy harvesting techniques, we are observing an impressive increase in the use of wearable devices. Kinetic human energy harvesting is the most efficient and practical method to power them reducing the need of batteries replacement since walking or running is how humans already expend much of their daily energy. The present energy harvesting technologies still have several limitations. In this work, thanks to a mechanical framework specifically designed to reproduce the kinematic of a knee joint and actuated using recorded human motion patterns, we demonstrate the feasibility of the non-resonant employment of the Macro Fiber Composites (MFCs) to scavenge energy from the various human body movements. Both the energy of periodic and aperiodic motions can be harvested. The electrical characteristics of the whole system focusing on the maximum power point of the MFC have been investigated to optimize the system power output.

Index Terms—Energy harvesting, Macro Fiber Composite, Piezoelectric fibers, Wearable, Human motion, Body sensor network.

I. INTRODUCTION

THE remarkable progresses in science and technologies over the past decades are making us increasingly dependent on portable electronic devices [?]. With the advances being made in wireless technology and low power microelectronics, we are observing a dramatic growth of interest for wearable technology [?], [?].

Smart wearable systems, also named as Wireless Body Area Networks (WBANs), are wireless networks used for communication among sensor nodes operating on, in, or around the human body in order to monitor vital body parameters and movements. WBAN enables ubiquitous monitoring of a person and they are increasingly used in several applications such as health-care, well-being, sport, entertainment, assisted living, protection and safety. [?], [?], [?], [?], [?], [?] Low power microelectronics and power management approaches to minimize the energy consumption while meeting required performance constraints, are going to have considerably effects on the everyday used devices. For instance, Magno et al. [?] developed a low power WBAN platform focusing on the minimization of the power consumption. The possibilities of switching off the sensors and even the main radio while the ultra low power wake up radio keeps listening for asynchronous commands allow to significantly reduce the power consumption, achieving even $1.8 \mu W$ in deep sleep. Power

autonomy of the sensor nodes is essential for their success, and this requires, beyond the development of low-power electronics, the research of long-life energy sources. Nowadays the majority of the devices are powered by batteries, which dominate weight, size and need to be constantly charged. Therefore, it is necessary to encourage different power sources. There are four possible ways to realize a distributed sensor network with adequate performance, as following: enhance the energy density of the storage systems; reduce the power consumption of the sensor; develop self-powered sensors by generating or harvesting energy; or transmit the power from a centralized source to the sensor. Among these various possible solutions the most efficient and practical method is to develop self-powered sensors by harvesting energy from the nearby available energy sources [?], [?]. There are few sources from which we can harvest energy for wearable wireless sensors, among them we can point to kinetic energy harvested from the human body motion [?], [?].

Among human activities, walking has the greatest potential for mechanical energy harvesting. It is indeed a routine activity which involves legs, upper limbs and center of mass motion. Therefore, knees, ankles, shoulder and elbow joints are promising targets for energy harvesting while walking. One possible division is to distinguish between active and passive energy harvesting methods. The active powering of electronic devices takes place when the user has to do a specific activity in order to power the product, on the contrary the passive powering takes place when the user does not have to do any task different from the normal use of the product. For instance, the self-winding watch, which utilizes the motion of the user's arm to accelerate a small internal mass, produces 1 mW when it is vigorously shaken and $5 \mu W$ when the watch is worn [?]. The energy output of active powering is often greater than that of passive powering, but this is at the cost of fully employing the user's attention and strength, so passive energy harvesting methods, in which the energy is harvested from the user's everyday actions, needs to be investigated more deeply. Various devices have been developed to harvest energy from human motion [?], [?]. They can be grouped into three categories based on the principle used in their energy conversion: inertia-based harvesters; impact force-based harvesters; and motion driven harvesters. The inertia-based harvesters use the inertia force of a proof mass, e.g. the suspended-load backpack that converts mechanical energy from the up-and-down movement of the carried load when walking. It generates 7.4 W during fast walking carrying a 38 kg load [?]. The impact force-based harvesters use the forces from a large moving mass (e.g. body weight) and the research

Authors are with the PERCRO laboratory of TeCiP Institute, Scuola Superiore Sant'Anna, Pisa, Italy e-mail: (n.lastname@sssup.it).

Manuscript received XXXX, 2016;XXXX.

is especially focused on harvesting the heel strike collision energy which is estimated to be up to hundreds of mW, as the device that use an electroactive polymer generator inserted into the shoe heel to harvest 0.8 W electrical [?], [?], [?].

The most promising energy harvesting method is the motion-driven harvester that harness electricity directly from limb motion. For instance, the 1.6 kg knee energy harvester generates 2.5 W per knee at a walking speed of 1.5 m s^{-1} [?] selectively engaging power generation at the end of the swing phase. Among the aforementioned energy harvesting technologies, the suspended load backpack and knee-mounted energy harvester produced the largest amount of power, making them suitable for powering portable devices with a higher power requirement. However, these technologies still have several limitations: they need the user to carry a cumbersome and heavy load that cause additional metabolic cost. There is a great need of new technologies to harvest biomechanical energy without creating discomfort to the users. The development of effective, reliable and low-cost sensors for the human body with embedded power generation needs relevant innovation in optimizing the efficiency of power harvesting from human energy sources, which are generally irregular and small. Given the irregular nature of these sources, an improvement of energy harvesting efficiency requires novel materials and methods for energy transductions to be investigated and validated. Under this perspective, recently developed composite materials, thanks to the aid of piezoelectric fibers [?], [?], [?], show relevant advantages with respect to rigid and fragile traditional piezoceramic sheets [?], [?]. This is the case of Macro-Fiber Composites (MFCs) tested in our works. MFCs have been developed at the NASA Langley Research Center [?] and are currently commercialized by Smart Material GmbH, Dresden, Germany [?]. Nowadays, MFC can be found commercially in the two operation modes: MFC with interdigitated electrodes to induce a longitudinal mode in the fibers (d_{33} -mode, denoted by MFC P1-type); and MFC with netlike electrodes on top and bottom to impress an electric field in the thickness direction of the MFC, thus using the transverse mode in the fibers (d_{31} -mode, denoted by MFC P2-type) [?]. Alternative design using the fibers shear mode (d_{15} -mode) have been proposed [?], but are not yet commercially available. Compared to the traditional piezoelectric materials such as lead zirconate titanate (PZT), the MFC are characterized by their flexibility on large deformation, which enables them to harvest energy directly from large bending motions with little brittle fracture risk and long lifespan. This approach is especially suited to harvest energy from human body motion given that exploiting their resulting vibrations would entail a resonant employment of the piezoelectric transducer which often causes issues in developing damping systems in wearable devices [?]. In our preliminary work [?], we proposed a method to evaluate the order of magnitude of MFC power output, thanks to a mechanical framework specifically designed to replicate the kinematic of a knee joint and actuated using recorded human motion patterns belonging to walking and running activities. To the authors knowledge, at the state of the art there are no studies investigating the possible differences between the MFC power outputs of periodic and aperiodic human motions under

non-resonant bending conditions.

As every moving object in nature, the human body movements can be classified into periodic and aperiodic, the former are motions that recurs over and over the same, instead the latter are not occurring at regular intervals. Given the significant difference between them, after having introduced the analysis of the power outputs of some periodic actions [?], it has been necessary to investigate the power outputs achievable with aperiodic motions, and compare them to understand the main parameter(s) influencing the power output amount.

To this end, in this work we analyzed a higher number of periodic motions with wider frequency range and a great variety of aperiodic activities. Furthermore, in this paper we experimentally investigate the electric characteristics of the MFC patch focusing on the maximum power point (MPP) because even if in first approximation [?] it can be considered fixed, we have shown that the electric load need to be adapted to the mechanical input to optimize the energy harvester power output.

Among the different wearable locations, we have been targeting the bending of the knee as energy source because it is identified as one of the more promising opportunities to harvest energy from the body [?]. Advantages of knee bending include the motion amplitude (120° minimum angular range), the imposed frequency, and its frequent use in everyday life, given that walking or running is how humans already expend much of their daily energy. After the introduction, the paper is organized as follows. In Section II we give a description of the energy harvesting system, and a presentation of the experiments is given in Section III. The results are presented in Section IV and discussed in Section V. Finally, the conclusions of the study are presented in Section VI, along with an examination of possible future works and improvements.

II. MATERIALS

A non-resonant energy harvesting mechanism with wide operation frequency band is investigated for collecting energy from low-frequency human joint motion, both periodic and aperiodic. The energy harvesting system (Figure 1) is composed of the P2-type MFC piezoelectric patch (active area of $85 \times 28 \text{ mm}^2$ and thickness of 0.3 mm), attached to a mechanical structure purposely-built to reproduce human joints motion approaching one degree of freedom, as elbow or knee. The structure is actuated by a DC motor thanks to an ARM microcontroller board along with the motor driver and a 8 channel logic analyzer to acquire the MFC's power output. The MFCs are planar piezoelectric devices which combine the energy density of piezoceramic materials with the flexibility and durability of epoxy. They consist of a sheet of aligned rectangular piezoceramic fibers embedded in an epoxy matrix, which inhibits crack propagation, and sandwiched between electrodes. The P2-type MFC [?] is especially suited for energy harvesting applications due to netlike electrodes that induce a transverse mode in the fibers and grant a higher capacitance and increased charge generation at the same strain level compared with the P1 device (Table I). Thus, it allows to harvest energy from large bending motions without reliability

TABLE I
COMPARISON BETWEEN MFC P1 AND P2 TYPES

MFC devices	Operation Voltage (V)	C (nF/(cm) ²)	d ₃₃ (pC/N)	d ₃₁ (pC/N)	Strain/Volt (μstrain/V)	Charge/Strain (pC/ppm)
P1	-500/+1500	0.42	460	-	0.7..0.9 [0...1500V]	1670 [>100V]
P2	-60/+360	4.5	-	-370	-2 [0...360V]	3250 [<100V]

(a)
CAD
model
of
frame

(b)
Mounted
test
setup

Fig. 1. Test setup with the 3D printed mechanical frame, the patch mounted and electrically connected and the electrical motor.

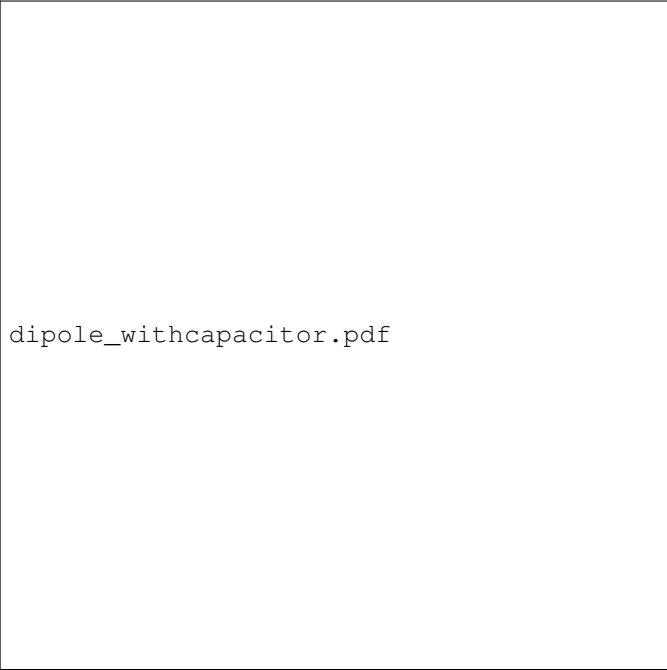
limitations. To test the MFC power output from specific human activities under non-resonant bending conditions, in our previous work [?] we developed a mechanical framework specifically designed to reproduce the kinematic of a knee joint and actuated using recorded human motion patterns. The mechanical frame has been designed in SolidWorks (Figure 1a) and printed with a 3D printer (Figure 1b). Besides the main fixed frame, it is composed of a revolving frame that allows the MFC patch bending, a rail to let the patch slide into, and the motor frame. There are two limit positions to avoid the patch to be over-bent: when the revolving frame is in vertical position the patch is straight into the rail, and moving until the max bending stop, energy is generated. The peculiar coupling between the revolving frame and the rail allows the MFC patch to be bended without stretching, thus preventing the risk to break it. We actuated and sensed the structure with a Maxon motor modular system composed of a DC brushed motor and an encoder to monitor the patch bending-angle. They are both connected to the circuit board: an ARM microcontroller STM32F407VGT6 Cortex-M4 32-bit RISC, 168 MHz (ST Microelectronics, Italy) integrated with a VNH5019 motor driver (Pololu, Las Vegas, NV), a fully integrated H-bridge that can be used for bidirectional speed control of the motor. Given that human movements cover a wide frequency and amplitude ranges and accordingly the voltage output levels of the MFC patch can be very different, it is not possible using the STM board analog-to-digital converter. In order to obtain a trustworthy output power, the patch voltage output is acquired by an 8 channel logic analyzer (Logic Pro 8, Saleae, San Francisco, CA) with each analog input, that saturates outside the range ±10V and has a protection for signals within ±25V for continuous operation, connected to a PC via USB. The DC motor position control is a Proportional-Integral-Derivative (PID) kind integrated in a dedicated interface to program the ARM microcontroller board implemented in MATLAB Simulink R2013b (Mathworks, Natick, MA).

III. METHODS

Since every energy harvesting system combines two different sub-systems, a mechanical one and electrical one, both have to be designed very carefully. Only if both interfaces match their direct connected environment, the mechanical load conditions, as well as the charge electronics input characteristics, a high degree and efficient harvesting of kinetic human energy can be observed. The majority of the kinetic energy harvesters are working in a resonance mode which requires a well-tuned mass/stiffness system for a high efficiency. However, a fact is that most mechanical vibration sources for energy generators show a broadband behaviour. Therefore, several harvester systems with different resonance frequencies would be necessary to improve the total system efficacy thus increasing the device complexity and cost. In addition, the damping systems to the natural frequency of the harvester are bulky and often cause inconveniences to the user [?], [?], [?], [?]. Therefore, the mechanical sub-system, which we have already described in the previous Section, is specifically designed to directly attach the MFC patch to the area of maximum strain allowing to work in an off-resonance mode. This approach permits to harvest energy from the entire range of motion frequencies independently of resonance restrictions. Considering the electric part of the harvester, in Figure 2 the electrical representation of the MFC patch is reported. Basically, the Maximum Power Point (MPP) is obtained when the external impedance equals the internal impedance. In a first approximation the MFC could be represented as an ideal energy source with only the internal resistance represented in Figure 2 and in case of linear source and load, the MPP will occur only at the operating point in which the external load resistor (R_{out}) equals the internal resistor (R_{in}) of the piezoelectric material. In this case, the inner impedance of the piezoelectric patch can be considered fixed and as a consequence also the optimal impedance load. In this work, differently from the previous [?], a more realistic electrical equivalent circuit of the MFC has been used (Figure 2) [?]. It includes an internal capacitance (C_{in}) in parallel to the internal resistance (R_{in}), beyond the ideal AC sinusoidal voltage source (V_q). Therefore, the MPP impedance load is affected by the operating frequency. As reported in [?], from the equivalent circuit in Figure 2, the total internal impedance, Z_{in} can be represented as the relation between the resistive impedance, $Z_R = R_{in}$ and the capacitive impedance, $Z_C = 1/j\omega C_{in}$:

$$Z_{in} = \frac{Z_C Z_R}{Z_C + Z_R} = \frac{R_{in}}{1 + 2j\pi f R_{in} C_{in}} \quad (1)$$

It is clear that the MPP varies according to the operating frequency. According to Equation 1, at high operating frequencies



dipole_withcapacitor.pdf

Fig. 2. MFC electric representation.

the MPP resistance can be approximated by Equation 2, i.e. it is inversely proportional to C_{in} and to the operating frequency.

$$R_{out_peak} = |Z_{in}| = \frac{1}{2\pi f C_{in}} \quad (2)$$

Therefore, we performed some tests to verify this behaviour and to detect the best load value considering the frequencies of the human motions selected to be tested. As reported in Section IV-1, we chose 16 different resistances in the range from 120 k Ω to 4.9 M Ω and we evaluated the power outputs actuating the energy harvesting system with 30 $^\circ$ and 45 $^\circ$ amplitudes sinusoidal waveforms each of which at four different frequencies: 0.5 Hz, 1 Hz, 1.5 Hz and 2 Hz, for a total of 128 trials. After having established the overall setup, we gave thought to the motor control input. In this work no experiments with humans have been performed. We extracted human motion data from the Carnegie Mellon University (CMU) motion capture database [?], a free dataset of motions classified by subject number or motion category. It is composed of several different human activities that can be grouped into five main categories: human interaction between two subjects; interaction with environment as climbing or walking on an uneven terrain; locomotion as walking, running or jumping; physical activities and sports, for instance basketball or skateboarding; and situations and scenarios as communication gestures or pantomime. The motion data are recorded by means of a marker-based motion capture system, the Vicon motion capture system [?] (OMG, plc.) consisting of 12 infrared MX-40 cameras, each of which recorded at 120 Hz with images of 4 Mpx resolution. Motions are captured in a working volume of approximately 3x8m and the capture subject wears an adherent black jumpsuit with 41 markers taped on. The Vicon cameras see the markers in infra-red and the images that the various cameras pick up are triangulated to

get 3D data. The 3D data obtained can be arranged in different ways: Marker positions mode: the file contains the 3D marker positions data (file .c3d) that can be relatively clean, but the user has to figure out how each marker is related to the other; Skeleton movement mode: data can be organized in two ways, the .vsk/.v pair or the .asf/.amc pair. The former element of the pair describes the skeleton and its joints, their connections, lengths, degrees of freedom, and mathematical transformation. The latter element of the pair contains the movement data. The .asf/.amc pair are derived from the .vsk/.v pair with the Vicon software (Vicon BodyBuilder), specifically designed to make the implementation of biomechanical models. We fused and extracted the knee flexion position data, to control our motor and simulate the motions to test in term of harvestable energy, from the skeleton movement .asf/.amc pair because, in spite of being binary as the .c3d and the .vsk/.v files, they are ASCII, a format easy to parse and to work with. Moreover, the angles are already in Euler angles format. For actuating the energy harvesting system we selected 29 actions from the CMU motion database, 15 periodic and 14 aperiodic, obtaining overall 62 knee motion trails to test. This allowed our tests to benefit from considerable variability, as people do not move symmetrically and have different styles in terms of different motion amplitude and frequency values, even between the two knees of the subject in the same trial. The periodic motions (Section IV-2), spanning frequencies from 0.8 Hz to 2.3 Hz and motion amplitudes from 60 $^\circ$ to 115 $^\circ$ (Figure 3a), belong to 12 subjects with different style of walking, marching, running, and jogging. The aperiodic motions selected (Section IV-3) span motion amplitudes from 33 $^\circ$ to 117 $^\circ$ (Figure 3b) and belong to 9 subjects doing different activities, as soccer kicking, jumping, playing baseball or basketball, skateboarding or more common activities such as getting up from chair. In Figure 4, where the Power Spectral Densities (PSD) of the periodic and aperiodic actions selected are reported, it can be seen that the knee joint movements do not have a fixed frequency and the strongest variations are in the range of 1-2 Hz.

IV. RESULTS

The output signals, the voltage drop across the optimum resistance and the angular position, are measured simultaneously by the 8 channel logic analyzer and by the microcontroller board acquisition system respectively, in order to correlate the output power with the angular position of the joint (Table ?? and III).

1) *Optimal resistance load assessment:* In piezoelectric transducers, the function describing the output power with reference to the applied load has an absolute maximum at each operating frequency (Figure 5). From Figure 5, it is evident the existence of different optimal resistances (R_{out_peak}) at each frequency. In addition, it can be seen that the 30 $^\circ$ four curves show lower levels of power output than the 45 $^\circ$ curves, and for each amplitude there is an upward trend in the power output as the frequency increases. Thus, both the higher frequency and the higher motion amplitude of the mechanical input cause higher power outputs. Figure 6a shows the relation between the optimal load resistance (R_{out_peak}) and frequency. It is found



(a) Maximal and minimal periodic motion amplitudes.



(b) Maximal and minimal aperiodic motion amplitudes.

Fig. 3. Motion amplitudes of the tested motion data: periodic (a) and aperiodic (b).

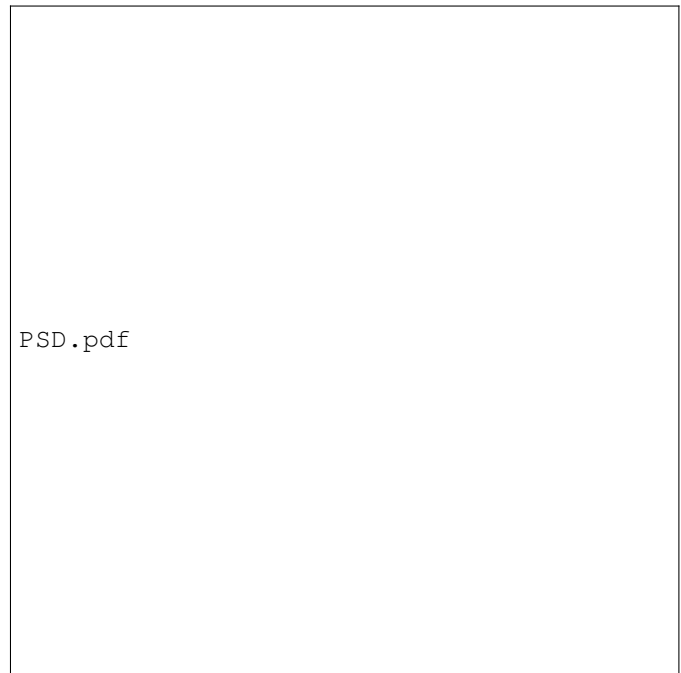


Fig. 4. Power Spectral Density (PSD) of periodic and aperiodic motions.

Fig. 5. Output power with reference to the applied resistance load with 30° and 45° amplitudes sinusoidal waveforms input (Alpha) at four different frequencies: 0.5Hz, 1Hz, 1.5Hz and 2Hz (Freq).

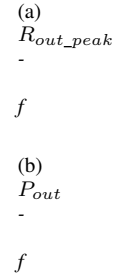


Fig. 6. Optimal resistance load (R_{out_peak}) (a) and electrical power output (P_{out}) (b) with regards to the sinusoidal input frequency (f).

that, if the mechanical input has a varying frequency the inner impedance of the piezoelectric patch cannot be considered fixed, even at low frequency. The higher the input frequency the lower the optimal load resistance value. Besides seeing the downward trend of the optimal load with the frequency, from Figure 6a it can also be seen that the higher the input motion amplitude the lower the optimal resistance value is. Figure 6b depicts the relation between the power output and the sinusoidal input frequency. It is clear the connection between these two variables, the higher the operating frequency, the higher the power that could be harvested from the MFC. The result of an overall analysis on the 128 trials (Figure 7), averaging out the output powers at each resistance value, shows the typical waveform of a piezoelectric transducer output power with reference to the applied load, and allows to choose the resistance load ($R = 470 \text{ k}\Omega$) to use in the remaining tests.

Fig. 7. Relation between the average output power at each resistance value and the resistance loads.

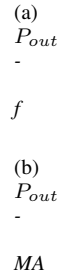


Fig. 8. Power output (P_{out}) with reference to the frequency (f) (a) and the motion amplitude (MA) (b) of the periodic CMU motions. In (b) outliers removed from fitting are highlighted by the green crosses.

2) *Periodic data assessment:* In Figure 8a, the power output with reference to the frequency of the 15 periodic CMU motions is reported. The smoothing spline interpolation method (p coefficient 0.9984105) is used because it provides a flexible way of estimating the underlying regression function using spline functions which are piecewise-defined by polynomial functions, and which possesses a high degree of smoothness at the places where the polynomial pieces connect. As expected, the power output has a peak around 1.5 Hz frequency (Figure 8a). This is due to the combined effect of the optimal resistance chosen, that gives a power output peak exactly at that frequency in the 45° case (Figure 6a), and the higher motion amplitude of those knee movements, between 85° and 114°, than the others (Table ??). The Sexy Lady Walk represents an exception. Although the amplitude of her knees' motion is big, the low motion frequency would require a higher optimal resistance to generate bigger power outputs. These exceptions are more evident in Figure 8b, where the power output, interpolated with the polynomial method (Equation 3), with reference to the motion amplitude, is reported.

$$f(x) = 0.02678 * x - 1.595 \quad (3)$$

It can be observed that the two outliers at 85° and 92° have definitely lower power outputs than the others with comparable motion amplitudes. The waveform illustrated confirms what we have already deduced from Figure 5, the electrical power output has an upward trend with the motion amplitude.

3) *Aperiodic data assessment:* The next figure (Figure 9) presents the electrical power outputs with regard to the angular speed in case of periodic (9a) and aperiodic (9b) motions. The non-linear least squares method is used to interpolate the data with the following equations:

$$f(x) = 0.03263 * x^{1.964} \quad (4)$$

$$f(x) = 0.1097 * x^{1.142} \quad (5)$$

Equation 4 refers to the fitting equation computed for periodic motions and equation 5 is the fitting equation computed for aperiodic motions. Although the aperiodic motions have lower power output levels (Table III), both have an upward trend with the angular speed. The previous fitting equations could

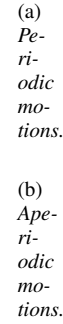


Fig. 9. Electrical power outputs with regards to the angular speed (Ω) in case of periodic (a) and aperiodic (b) motions.

be used as starting points to develop an analytical model of the MFC patch.

V. DISCUSSION

The majority of the biomechanical energy harvesters work in resonance mode [?], [?] and are not appropriate to scavenge energy from the unpredictable human body movements. Thus, we designed an off-resonance energy harvesting transduction system purposely built to effectively extract energy in a wide range of frequencies, motion amplitudes, and bending velocities. The innovative electromechanical transducer developed allows to reach power output levels sharply over those of similar devices [?] currently at the state-of-the-art in research on piezoelectric energy harvesting systems exploiting human joints motion. For instance, by considering the flexion-extension motion of the 9th subject knees associated to the run activity at 1.35 Hz frequency with 112° motion amplitude and an angular velocity of 6 degs⁻¹, we obtained about 1.5 μW (Table ??); and by employing two MFC flexible patches per knee, one in the front and one on the back of the joints, a total 6 μW output power can be achieved. In the previous work [?] we investigated the energy output of 8 periodic actions and we deduced that the main parameter influencing the energy harvesting power output is the motion amplitude rather than the frequency. This study confirms those results, adding an important consideration on the dependence of the power output on the frequency.

The new optimal resistance load assessment (Section IV-1) highlights that, even if the MFC patch is directly attached to the maximum deformation surface and it works in an off-resonance mode, the mechanical input frequency influences the power output. It entails, together with the motion amplitude, a variation of the MFC impedance that can cause a mismatch between the internal and the load impedances taking down the power outputs.

The in-depth evaluation of the power outputs carried out in this work, for both periodic (15 actions) and aperiodic (14 actions) mechanical inputs, underlines the importance of the joint angular velocity in the power output maximization. The power outputs of the periodic motions are higher than the aperiodic ones because they have higher bending velocities than the aperiodic motions chosen (Table ?? and III). This is apparent looking at subject 141 knees' motion during a Step

TABLE II
EXPERIMENTAL TEST RESULTS OF THE 15 PERIODIC CMU MOTIONS [?].

CMU_name	Action	Amax (deg)	f (Hz)	Omega (deg/s)	Vavg (V)	Iavg (uA)	Pavg (uW)
06_01_Left	Walk	62.6	0.82	1.90	0.181	0.386	0.140
05_01_Left	Fast Walk	61.1	1.66	1.93	0.196	0.416	0.143
35_01_Left	Walk	59.7	0.87	2.22	0.184	0.393	0.150
35_01_Right	Walk	62.5	0.85	2.16	0.190	0.403	0.151
05_01_Right	Fast Walk	62.8	1.65	2.14	0.198	0.420	0.153
137_29_Right	Strong Man Walk	72.8	0.85	2.21	0.196	0.416	0.156
137_38_Left	Sexy Lady Walk	85.1	0.58	1.69	0.163	0.350	0.156
137_38_Right	Sexy Lady Walk	92.1	0.59	1.73	0.180	0.383	0.170
137_29_Left	Strong Man Walk	73.7	0.90	2.45	0.210	0.450	0.188
08_01_Right	Walk	61.2	0.98	2.78	0.225	0.479	0.190
12_02_Left	Walk	76.2	0.76	2.23	0.222	0.472	0.204
06_01_Right	Walk	68.8	0.82	2.32	0.223	0.475	0.220
12_02_Right	Walk	80.0	0.76	2.44	0.244	0.520	0.245
08_01_Left	Walk	72.4	1.98	3.33	0.255	0.544	0.250
07_12_Right	Brisk Walk	74.5	2.28	3.62	0.271	0.576	0.286
138_01_Right	Marching	70.7	0.82	2.68	0.280	0.594	0.320
16_36_Right	Run	73.7	1.22	4.30	0.301	0.641	0.321
16_36_Left	Run	70.9	1.22	4.12	0.310	0.657	0.345
138_01_Left	Marching	75.6	0.81	2.91	0.307	0.653	0.396
07_12_Left	Brisk Walk	72.6	2.29	3.70	0.315	0.670	0.475
35_26_Right	Run/Jog	86.3	1.46	5.21	0.450	0.953	0.704
35_26_Left	Run/Jog	89.1	1.40	5.20	0.466	0.992	0.745
02_03_Right	Run/Jog	83.5	1.34	4.61	0.459	0.978	0.799
127_07_Left	Run	85.7	1.52	5.25	0.487	1.040	0.830
02_03_Left	Run/Jog	87.5	1.40	5.10	0.495	1.053	0.865
09_02_Right	Walk/Wonder	99.9	1.40	6.03	0.490	1.042	0.990
127_07_Right	Run	99.1	1.52	6.80	0.524	1.114	1.007
09_06_Left	Run	113.9	1.40	6.51	0.634	1.349	1.455
09_02_Left	Walk/Wonder	106.5	1.34	6.00	0.605	1.287	1.469
09_06_Right	Run	112.5	1.34	6.32	0.612	1.320	1.484

TABLE III
EXPERIMENTAL TEST RESULTS OF THE 14 APERIODIC CMU MOTIONS [?].

CMU_name	Action	Amax (deg)	Omega (deg/s)	Vavg (V)	Iavg (uA)	Pavg (uW)
124_01_Right	Baseball Pitch	33.8	0.52	0.045	0.095	0.010
114_04_Right	Getting up from chair	83.2	0.50	0.054	0.115	0.020
114_04_Left	Getting up from chair	86.0	0.48	0.086	0.182	0.034
134_06_Right	Skateboarding - Push Turn Left	43.2	0.83	0.083	0.176	0.034
10_05_Right	Soccer Kick	56.4	1.40	0.096	0.205	0.054
140_09_Right	Get Up From Ground Laying on Back	114.9	0.75	0.115	0.245	0.073
140_08_Left	Get Up From Ground Laying on Back	107.8	0.47	0.124	0.265	0.092
140_09_Left	Get Up From Ground Laying on Back	111.2	0.60	0.120	0.253	0.094
124_11_Right	2 Foot Jump	72.2	1.49	0.151	0.321	0.108
118_02_Left	Jump	88.9	0.77	0.148	0.315	0.109
118_02_Right	Jump	87.2	0.83	0.157	0.334	0.113
139_17_Left	Get Up From Ground	106.7	0.85	0.177	0.377	0.121
139_17_Right	Get Up From Ground	117.3	0.79	0.175	0.372	0.124
140_08_Right	Get Up From Ground Laying on Back	111.3	0.56	0.178	0.378	0.135
124_06_Right	Basketball Lay Up	77.8	1.20	0.145	0.308	0.136
124_11_Left	2 Foot Jump	77.5	1.61	0.171	0.364	0.140
124_01_Left	Baseball Pitch	91.8	1.07	0.127	0.270	0.144
10_05_Left	Soccer Kick	69.0	1.55	0.168	0.358	0.158
134_06_Left	Skateboarding - Push Turn Left	73.8	1.70	0.173	0.369	0.166
124_06_Left	Basketball Lay Up	84.4	1.38	0.139	0.296	0.167
118_05_Right	Jump	91.6	0.76	0.215	0.457	0.183
118_05_Left	Jump	94.5	0.82	0.222	0.472	0.202
16_01_Right	Jump	67.0	1.37	0.233	0.495	0.206
134_05_Right	Pump Jump	78.7	2.13	0.230	0.488	0.222
16_01_Left	Jump	64.5	1.38	0.265	0.563	0.237
134_05_Left	Pump Jump	115.3	3.00	0.264	0.563	0.370
141_09_Left	Step Over	85.8	4.06	0.250	0.529	0.420
141_09_Right	Step Over	106.0	5.16	0.376	0.800	0.824

Over. In this case the knees' bending speed was comparable to periodic motions' ones and the obtained power output turned out to be in the same order of magnitude ($0.8 \mu W$). Taking into account the energy requirements for WBAN discussed in the introduction (e.g. [?]), even if the power outputs are in the range of the μW , developing an electrical circuitry to temporarily accumulate the energy generated in a small storage battery or supercapacitor would allow the integration of our energy harvesting transduction system developing a zero-power WBAN able to autonomously monitor different physiological parameters.

VI. CONCLUSIONS

The new energy harvesting transduction method described is a valid starting point to grow a zero-power wearable device for monitoring people anywhere and at anytime. Collecting mechanical energy produced by human joint motion with such thin piezoelectric patch will allow everybody to extract his power without having to deal with current biomechanical energy harvesting system constraints such as the need to wear specific shoes or to carry a cumbersome and heavy load. Indeed, the main innovation of this work is the non-resonant employment of the piezoelectric transducer capable to scavenge energy from the unpredictable human body movements. Both the energy of periodic and aperiodic motions can be harvested given that the bending velocity is the critical parameter in maximizing the power output. The subject wearing the device is not bound to walk or jog at a specific frequency, whatever activity involving the knees bending will produce energy. In the near future an investigation on the relationship of the internal impedance of the MFC patch on both the frequency and the motion amplitude evaluating possible relations between them will be conducted. Furthermore, future developments will focus on the design of an automatic selector of the optimal load according to the mechanical input characteristic to match the internal and the load impedance thus maximizing the power output in every conditions. The development of non-linear techniques, such as Synchronized Switch Harvesting on Inductor (SSHI) or Synchronous Electric Charge Extraction (SECE), would have the potential to increase even more the output power. Furthermore, a wearable setup will be developed in order to evaluate the harvestable energy from real human activities along with the development of an ultra-low-power sensing system for human motion detection. The data used for this experiment are available at <http://dx.doi.org/10.21227/H2CD31> with source code on https://github.com/eruffaldi/paper_mfc_harvest.

CONTRIBUTIONS

Study concept: ER, GB. Study design: GB, ER, AF. Study Implementation: GB, AF. Acquisition of data: GB. Analysis and interpretation of data: GB, ER, AF. Drafting of manuscript: all.

ACKNOWLEDGMENT

The research was supported by TELECOM Italia.



Giulia Bassani is Research Collaborator at PERCRO Laboratory, TeCIP Institute, Scuola Superiore Sant'Anna (SSSA) and she received the PhD in Emerging Digital Technologies at SSSA and MSc degree in biomedical engineering from the University of Pisa in 2012. She participated the ICTIP - Inducement Prizes Design for Innovation and Entrepreneurship (H2020 CSA). She is currently within the Intelligent Automation Systems division at PERCRO and her research interests include the embedded wearable energy harvesting systems.



Alessandro Filippeschi is Assistant Professor at PERCRO Laboratory, TeCIP Institute, Scuola Superiore Sant'Anna. Alessandro is a mechanical engineer and he received a PhD in Perceptual Robotics at Scuola Superiore Sant'Anna in 2012 discussing a thesis on multimodal interfaces for sport training. He participated the FP7 EU projects SKILLS and REMEDI as well as the H2020 project Ramcip. He is co-founder of Wearable Robotics S.r.L. His research activity deals with human performance capture and analysis as well as the design of robotic haptic interfaces for human robot interaction. He is author of 8 papers on ISI-Journals and 26 conference papers.



Emanuele Ruffaldi is Assistant Professor at PERCRO of Scuola Superiore Sant'Anna. He received the PhD in Perceptual Robotics from SSSA in 2006. Inside PERCRO he is leading the group "Sensing, Modelling and Learning for Humans". He is PI of the H2020 robotic project RAMCIP, FP7 project PELARS, participating to FP7 REMEDI, and was WP leader in IP SKILLS. His research interests are in the field of virtual environments for robotics, machine learning and Human-Robot interaction. He has published 18 papers on ISI Journals, 10 book chapters, 90 conference papers. He is serving as Dissemination Chair of IEEE TC on Haptics.